PHYSICAL REVIEW C **88**, 041305(R) (2013)

Extreme nonstatistical effects in γ decay of ^{95}Mo neutron resonances

P. E. Koehler,[1,*] A. C. Larsen,[1] M. Guttormsen,[1] S. Siem,[1] and K. H. Guber[2]
[1]*Department of Physics, University of Oslo, N-0316 Oslo, Norway*
[2]*Reactor and Nuclear Systems Division, Oak Ridge National Laboratory, Oak Ridge, Tennessee 37831, USA*
(Received 27 June 2013; revised manuscript received 6 September 2013; published 23 October 2013)

We demonstrate that high-quality total radiation width (Γ_γ) data are a virtually untapped resource for testing and improving nuclear models. To this end, we obtained unprecedentedly large sets of Γ_γ values for all six s- and p-wave J^π values for ^{95}Mo neutron resonances. We show that Γ_γ distributions simulated in the framework of the nuclear statistical model are in sharp disagreement with the data. Simulations modified to include doorway effects resulted in much better agreement. These results call into question the reliability of the nuclear statistical model.

DOI: 10.1103/PhysRevC.88.041305 PACS number(s): 24.30.Gd, 24.60.Dr, 24.60.Ky, 25.40.Lw

There has been significant controversy surrounding γ decay of molybdenum isotopes below the neutron separation energy. Widely different shapes for the photon strength function (PSF), representing the decay strength as a function of γ-ray energy, have resulted from various measurements [1–3]. In addition, the enhancement in strength at low γ-ray energies reported for molybdenum isotopes [1,2] has been called into question [4,5], although more recent data [6] strongly support its existence. There is also disagreement about the nature of γ decay following neutron capture on molybdenum isotopes. On the basis of a very few measured total radiation widths Γ_γ, it was suggested [7] that significant nonstatistical effects affected this decay. In contrast, it was found that the extreme statistical model was in very good agreement with two-step cascade γ spectra following thermal neutron capture [4] as well as coincidence-pulse-height spectra and other data for neutron-resonance capture [5].

Resolving these controversies is of central importance for applications such as advanced nuclear fuel cycles [8] and astrophysical nucleosynthesis studies. For example, the PSF shape can have substantial impact on astrophysical reaction rates [9] in explosive environments, and therefore significantly impact the resulting nucleosynthesis. In addition, as the nuclear statistical model is used to calculate almost all rates for nuclides beyond the reach of current experiments, it is important to test basic assumptions of this model.

Total radiation widths of neutron resonances represent a virtually untapped source of data in this endeavor. Due to the very large number of levels below the neutron binding energy B_n, there are thousands of channels by which γ decay can occur following resonance neutron capture, a few of which are schematically illustrated in Fig. 1. Hence, energies E_γ of these transitions span the entire range of level density (LD) and PSF below B_n. The total radiation width Γ_γ is the sum of all the partial widths for the initial (primary) γ transitions from the resonance.

According to the statistical model, strengths of each of these primary transitions follow the Porter-Thomas distribution (PTD) [10], with average strength proportional to the PSF (with an appropriate energy factor, which is E_γ^3 for dipole transitions) at the corresponding energy. It is further assumed that all, or at least the vast majority, of the channels are independent. Because the PTD is a χ^2 distribution with one degree of freedom ($\nu = 1$), the distribution of n independent samples from the PTD is a χ^2 distribution with $\nu = n$ degrees of freedom, which for large n is very narrow. In practice, however, the effective number of channels is very much reduced because the vast majority of transitions are to levels at higher excitations, which have very small partial widths and so contribute almost nothing to Γ_γ fluctuations. Therefore, ascertaining the size of Γ_γ fluctuations expected for a given PSF/LD combination requires detailed simulations of the partial widths. However, it is expected that there should be enough channels remaining so that the Γ_γ distribution will still be narrow and, by virtue of the central limit theorem, nearly Gaussian in shape. Any substantial deviation from the expected shape is a likely signature of important nonstatistical effect(s). A given PSF/LD combination is further constrained by the average total width $\langle\Gamma_\gamma\rangle$.

We show herein that calculations of Γ_γ distributions for ^{95}Mo neutron resonances, employing available measured and theoretical PSF and LD models, all yield results much narrower than measured, indicating the presence of substantial nonstatistical effects. Furthermore, we show that calculations modified to include nonstatistical effects yield results in much better agreement with the data. These results cast doubt on the reliability of the nuclear statistical model, especially for extrapolations involving γ decay, and demonstrate that Γ_γ distributions are a virtually untapped resource for testing and improving nuclear models.

Measurements were made at the Oak Ridge Electron Linear Accelerator (ORELA) white-neutron-source facility [11]. Descriptions of the apparatus can be found in Ref. [12]. The ORELA was operated at a pulse rate of 525 Hz, a pulse width of 8 ns, and a power of 7–8 kW. Neutron capture measurements were made at a source-to-sample distance of 40.12 m with a pair of C_6D_6 detectors using the pulse-height-weighting technique, and were normalized via the saturated 4.9 eV resonance in the ^{197}Au(n,γ) reaction. Total neutron cross sections were measured on a separate flight path via transmission using a ^{6}Li-loaded glass scintillator

*Corresponding author.

 ©2013 American Physical Society

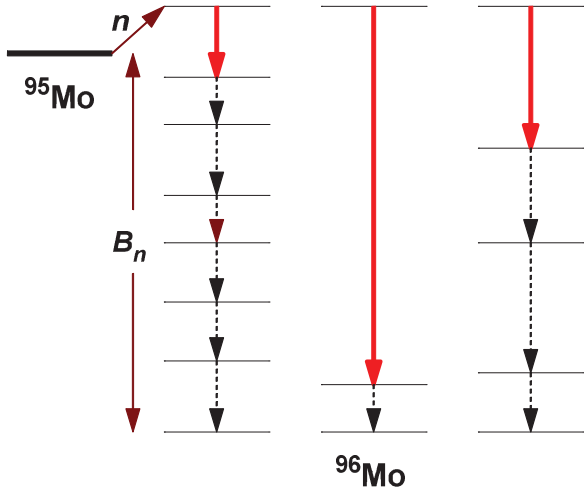

FIG. 1. (Color online) Schematic (not to scale) representation of γ decay following neutron capture in ^{95}Mo. In our experiments, resonance energies were less than 10 keV, which is negligible compared to $B_n = 9154.32 \pm 0.05$ keV for ^{95}Mo, and hence not included in the simulations. The total γ width Γ_γ determined in our $\mathcal{R}$-matrix analysis is the sum of the thousands of partial widths for all primary transitions, three of which are depicted as solid red arrows. Subsequent γ transitions, depicted by dashed black arrows, do not contribute to Γ_γ and hence are not part of the simulations.

at a source-to-detector distance of 79.83 m. Samples were metallic molybdenum, enriched to 96.47% in ^{95}Mo. Capture and transmission samples were 0.004591 and 0.02507 at/b thick, respectively.

For a quantitative comparison of experiment to theory, it is crucial to know the spins and parities of the resonances. Because the ground-state spin and parity of ^{95}Mo are $I^\pi = \frac{5}{2}^+$, s- and p-wave neutron resonances can have J^π values of 2^+, 3^+, and 1^-, 2^-, 3^-, and 4^-, respectively. Resonance spins and parities were determined using information contained in the γ-ray cascade following neutron capture, as described in Ref. [13]. A preliminary description can be found in Ref. [14]. A full report is forthcoming. The high quality of our resonance J^π determinations are illustrated in Figs. 2 through 4.

The technique is based on the fact that the γ cascade is dominated by dipole transitions, which limits spin changes to one unit for each step in the cascade. Hence, the higher the resonance spin, the more steps (higher multiplicity) needed in the γ cascade to the ground state. Therefore, higher spin resonances will have both softer singles spectra and a larger coincidence rate between γ detectors than lower spin resonances. In Ref. [13], a single ratio of singles counts, above a high threshold, to coincidence counts, with a lower threshold, was used to separate resonance spins.

We improved upon Ref. [13] by acquiring capture data in event mode and then using a computer code to choose gates on resonance singles and coincidence pulse-height spectra to optimize separation of spins and parities, in a bootstrap approach. It was found that in addition to the singles/coincidences ratio used in Ref. [13], the singles/singles and coincidences/coincidences ratios for different pulse-height regions also were sensitive to resonance spin and parity.

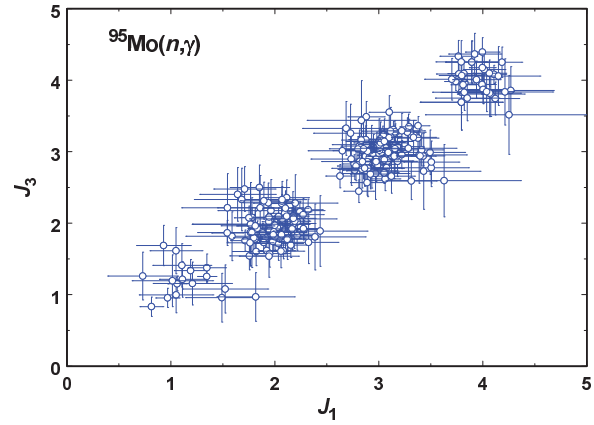

FIG. 2. (Color online) Two different spin indices calculated from singles and coincidence pulse-height spectra. J_1 was calculated from the ratio of counts in two different regions of the singles pulse-height spectra. J_3 was calculated from the ratio of counts in regions of the coincidence and singles pulse-height spectra. Open circles with (one-standard-deviation) error bars depict results for all resonances analyzed herein. Pulse-height ratios were scaled so that the data clusters would occur near integer values. See text for details.

Spin indices calculated from singles/singles and coincidences/singles ratios for resonances analyzed herein are shown in Fig. 2. Figure 3 shows a histogram of the weighted (by inverse variances) averages of the three spin indices. From these figures, it can be seen that resonance spins are very well determined. Figure 4 shows similar results for the separation of $J = 2$ and 3 resonances into the two parities.

As a result of this analysis, we were able to determine firm J^π assignments for 253 of the 314 observed resonances. This is a very large improvement over the 32 firm J^π assignments for the previously known 108 resonances. More importantly for the present work, we increased the number of resonances having both firm J^π assignments and Γ_γ values by almost a factor of 23; from 11 to 251.

The $\mathcal{R}$-matrix code SAMMY [15] was used to simultaneously fit our transmission and capture data and extract resonance energies, neutron widths, and total radiation widths. Plots of

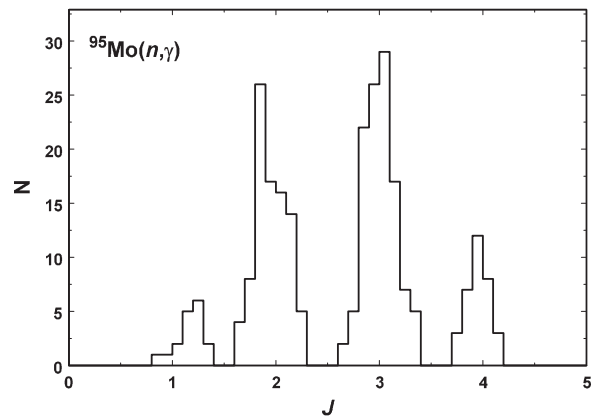

FIG. 3. Histogram of weighted averages of the three spin indices for resonances analyzed herein. Data for two of the three spin indices are shown in Fig. 2.

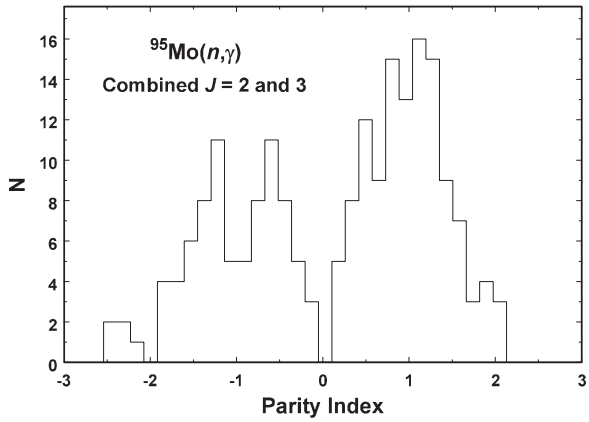

FIG. 4. Histogram of weighted averages of the three parity indices for resonances analyzed herein. Shown are the combined results for $J = 2$ and 3 resonances. Indices were scaled so that negative- and positive-parity resonances would cluster around -1 and 1, respectively.

the energy-reduced neutron widths, as a function of resonance energy, and cumulative Γ_γ distributions are shown in Figs. 5 and 6, respectively. To our knowledge, this is the first time that data of this quality and quantity have been obtained.

The veracity of our J^π assignments and the shape of our Γ_γ distributions are corroborated in several ways. For example, as expected from angular momentum penetrability, energy-reduced neutron widths for positive-parity resonance are, on average, constant as a function of neutron energy, whereas those for negative-parity resonances increase, on average, linearly with neutron energy. In addition, Γ_α values [16] for 2^+ resonances are much larger than those for 2^- resonances, as expected from Coulomb-barrier and parity-conservation considerations. Also, our data verify the previous nine firm 2^+ and 12 firm 3^+ assignments [17]. Furthermore, as shown

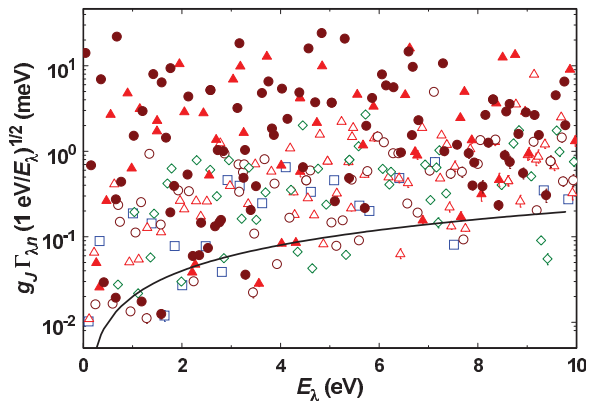

FIG. 5. (Color online) Energy-reduced values of observables $g_J\,\Gamma_{\lambda n}$ for ^{95}Mo neutron resonances λ at energies E_λ. The statistical factor for resonances having spin J is given by $g_J = (2J + 1)/[(2I + 1)(2j + 1)]$, where I and j are the target and neutron spin, respectively. Resonances assigned $J^\pi = 1^-$ are depicted as open blue squares, 2^- are open light red triangles, 2^+ are filled light red triangles, 3^- are open dark red circles, 3^+ are filled dark red circles, and 4^- are open green diamonds. A solid black curve indicates the threshold used to correct average resonance parameters for missed resonances.

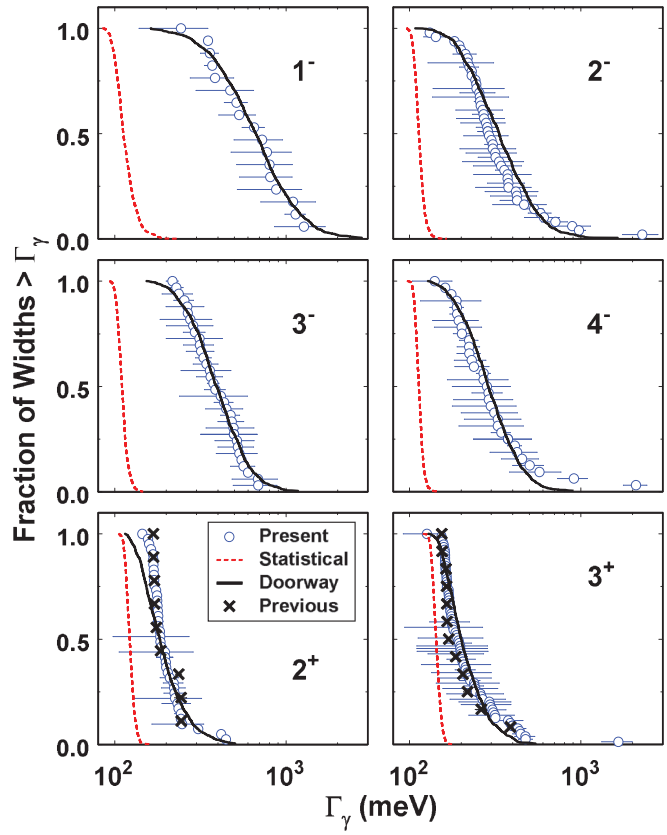

FIG. 6. (Color online) Cumulative Γ_γ distributions for ^{95}Mo + n resonances. Each panel shows the fraction of resonances having Γ_γ larger than a certain size vs the size. Data from the present work and those based on previous firm J^π values are shown as open blue circles and black x's, respectively. Error bars depict one-standard-deviation uncertainties as reported by SAMMY. Statistical-model simulations with and without an added doorway are shown as solid black and dashed red curves, respectively. Simulated Γ_γ values have been normalized by factors of 0.75, 0.9, 0.85, 1.1, 1.0, and 1.2 for 1^-, 2^-, 3^-, 4^-, 2^+, and 3^+ resonances, respectively. Not shown is the smallest 2^- Γ_γ (39.7 $\pm$ 2.9 meV).

in Fig. 6, the Γ_γ distributions for these resonances are in agreement with our more extensive data, verifying the essential broadness of the distributions. We also note that firm positive-parity assignments based on asymmetric resonance shape in our transmission data (an old, reliable technique) result in a combined 2^+ plus 3^+ Γ_γ distribution, which is as broad as the separate 2^+ and 3^+ distributions resulting from our new technique; hence, lending even further credence to our new results.

The statistical model assumes that partial radiation widths, $\Gamma_{\lambda\gamma f}(XL)$ of type X (electric or magnetic) and multipolarity L between resonance λ and final level f, follow a Porter-Thomas distribution (PTD) around their expectation value $\langle\Gamma_{\lambda\gamma f}(XL)\rangle$,

$$\langle\Gamma_{\lambda\gamma f}(XL)\rangle = \frac{f_{XL}(E_\gamma)E_\gamma^3}{\rho(E_\lambda, J_\lambda, \pi_\lambda)}, \qquad (1)$$

where $E_\gamma = B_n - E_f$ is the γ-ray energy, $\rho(E_\lambda, J_\lambda, \pi_\lambda)$ is the LD of resonances with spin J_λ and parity π_λ at energy E_λ, and $f_{XL}(E_\gamma)$ is the PSF for XL transitions.

The total radiation width Γ_γ of a neutron resonance (we drop subscript λ when referring to total widths for convenience and to maintain consistency with the literature) is given by the sum of partial radiation widths for all possible transitions to levels f below the neutron capturing state,

$$\Gamma_\gamma = \sum_f \sum_{XL} \Gamma_{\lambda\gamma f}(XL). \quad (2)$$

We simulated Γ_γ distributions using an approach very similar to the first step (primary γ decay) of the DICEBOXalgorithm [18], which has been used for simulations of γ-decay data from many different experiments (e.g., Refs. [4,5,17]). A complete level scheme (i.e., level energies E_f, spins J_f, and parities π_f), above a critical excitation energy E_c, was generated according to the adopted LD. Below $E_c = 2.50$ MeV, values of E_f, J_f, and π_f have been determined from experiments, and so were taken from Ref. [19]. Spin and parity selection rules were properly taken into account for individual transitions. Partial radiation widths $\Gamma_{\lambda\gamma f}(XL)$ for transitions from resonances λ to all possible final levels f were calculated by random sampling from PTDs characterized by expectation values given by Eq. (1).

Simulations were run using a variety of measured [1–3] and theory [20] LDs and PSFs. All LDs were normalized at the neutron separation energy to our measured value, $D_0 = 66.1 \pm 3.0$ eV, which was obtained by correcting the number of observed 2^+ and 3^+ resonances for threshold effects using the technique of Ref. [21], with the threshold shown in Fig. 5. For the measurements of Refs. [1,2], the spin distribution of Ref. [22] (which is parity independent) was used in this normalization. As this normalization affects both the LD and PSF slopes as well as the magnitude of the LD, both the shape and average value of the simulated Γ_γ distribution are impacted. This same LD also was used for simulations with the PSF of Ref. [3].

As the technique of Refs. [1,2] results in the total dipole PSF, it must be decomposed into $E1$ and $M1$ components. This decomposition, one example of which is shown in Fig. 7, was guided by current best knowledge of the relative sizes and shapes of the two components. Other possibilities, such as including the increase in strength at low energies in the $E1$ component, also were used in simulations. It was found that such changes had a relatively minor impact on the simulated Γ_γ distribution shapes. Other PSFs used in the simulations also are displayed in Fig. 7.

Simulated Γ_γ distributions using the LD and PSFs of Refs. [1,2] are shown as dashed red curves in Fig. 6, from which it can be seen that they are much narrower than the data in all cases. Simulations using all other LDs and PSFs described above also yielded distributions much narrower than the data. We also ran simulations using a χ^2 distribution with $\nu = 0.5$ degrees of freedom instead of the PTD. The resulting Γ_γ distributions were slightly broader than those simulated using the PTD, but still much narrower than the data.

Hence, our results verify the suggestion in Ref. [7], made on the basis of the wide distribution of a few measured Γ_γ values, that significant nonstatistical effects are present in the γ decay of Mo neutron resonances. Valence capture [23]

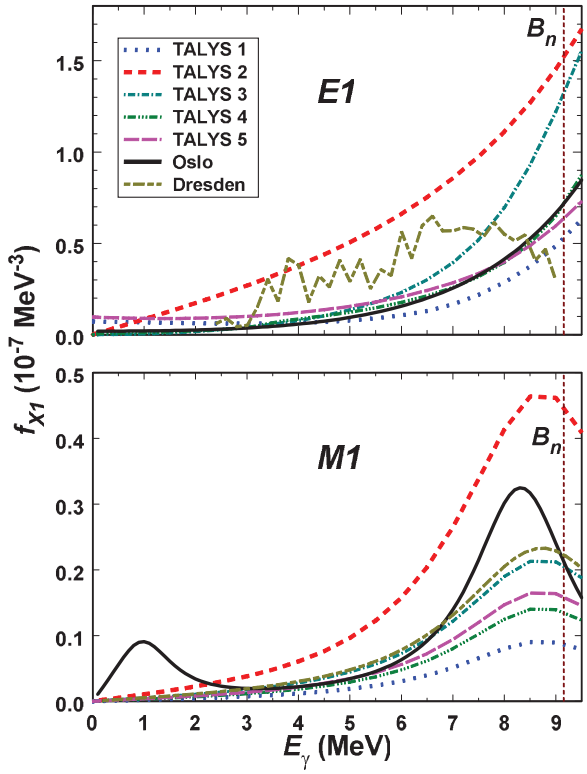

FIG. 7. (Color online) Different $E1$ (top) and $M1$ (bottom) PSFs used in the simulations. The first five curves represent theoretical models used in the code TALYS [20]. The solid black and long-short-dashed brown curves are from the measurements of Refs. [1–3], respectively. Location of the neutron binding energy B_n is indicated by the dashed vertical red lines.

was rejected as the source of these effects because calculated valence contributions were too small and because there was no significant correlation between neutron and γ widths as predicted by this model. With our much more extensive data, we also verify this latter contradiction to the valence model.

It was suggested in Ref. [7] that a doorway model might explain the wide range of measured Γ_γ values. However, no quantitative predictions for this model were available, which, to our knowledge, remains true today. The basic idea of a doorway model is that neutron-resonance wave functions, by virtue of the doorway, possess simple configurations which allow enhanced γ transitions, especially to levels at lower excitation that are simpler in structure. In the spirit of this model, we modified the simulations in the following way: A fraction f_d of transitions to excitation energies below some value E_d had their expectation values enhanced by a common factor F_e. Partial radiation widths for all transitions were still calculated by random sampling from PTDs characterized by their expectation values. Because a doorway might not affect resonances of all spins and parities in the same manner, in principle there could be different parameters for each J^π. In practice, it was found that $f_d = 1.0$, $F_e = 25$, and $E_d = E_c$ yielded results in reasonable agreement with all the data, as shown by the solid black curves in Fig. 6.

The question arises whether such a doorway mechanism is contradicted by the reasonably good agreement between

statistical-model-simulated and measured γ-ray spectra for two-step cascades following thermal neutron capture [4], and multiple-step cascades for resonance capture [5] on ^{95}Mo. As thermal capture does not proceed through a resonance, it may not be affected by the doorway. Also, the postulated factor-of-25 increase in the expectation values for the highest-energy transitions may have little effect on the simulated multiple-step cascade γ-ray spectra because such transitions are relatively rare. However, it may be interesting to search the data of Ref. [5] for possible signatures of the unusual nature of resonances in the tails of the Γ_γ distributions shown in Fig. 6. For example, of the spectra shown in Ref. [5], three correspond to resonances (E_λ = 708.3, 1296.9, and 1360.6 eV) which we have identified as having large Γ_γ values. The sum-energy spectrum is shown for only one (E_λ = 1360.6 eV) of these, and it is substantially different from the other resonances shown.

In summary, we have obtained an unprecedentedly large sets of total radiation widths of ^{95}Mo neutron resonances for all six s- and p-wave J^π values. We have shown that these data are in conflict with the nuclear statistical model and, furthermore, that substantial doorway enhancement results in reasonable agreement with all the data. These results call into question the reliability of the nuclear statistical model and demonstrate that Γ_γ-distribution data are a virtually untapped resource for testing and improving nuclear models.

This work was supported by the Research Council of Norway and by the Nuclear Criticality Safety Program and the Office of Nuclear Physics of the US Department of Energy.

[1] M. Guttormsen *et al.*, Phys. Rev. C **71**, 044307 (2005).
[2] M. Guttormsen *et al.*, arXiv:0801.4667v1.
[3] M. Erhard *et al.*, Phys. Rev. C **81**, 034319 (2010).
[4] M. Krtička *et al.*, Phys. Rev. C **77**, 054319 (2008).
[5] S. A. Sheets *et al.*, Phys. Rev. C **79**, 024301 (2009).
[6] M. Wiedeking *et al.*, Phys. Rev. Lett. **108**, 162503 (2012).
[7] A. R. de L. Musgrove, B. J. Allen, J. W. Boldeman, and R. L. Macklin, Nucl. Phys. A **270**, 108 (1976).
[8] Report of the Nuclear Physics and Related Computational Science R&D for Advanced Fuel Cycles Workshop, DOE Offices of Nuclear Physics and Advanced Scientific Computing Research (August 2006).
[9] A. C. Larsen and S. Goriely, Phys. Rev. C **82**, 014318 (2010).
[10] C. E. Porter and R. G. Thomas, Phys. Rev. **104**, 483 (1956).
[11] R. W. Peelle *et al.*, Technical Report No. ORNL/TM-8225, Oak Ridge National Laboratory (1982).
[12] P. E. Koehler *et al.*, Phys. Rev. C **62**, 055803 (2000).
[13] C. Coceva, F. Corvi, P. Giacobbe, and C. Carraro, Nucl. Phys. A **117**, 586 (1968).
[14] P. E. Koehler *et al.*, J. Korean Phys. Soc. **59**, 2088 (2011).
[15] N. M. Larson, Technical Report No. ORNL/TM-9179/R8, Oak Ridge National Laboratory (2008).
[16] W. Rapp, P. E. Koehler, F. Käppeler, and S. Raman, Phys. Rev. C **68**, 015802 (2003).
[17] S. A. Sheets *et al.*, Phys. Rev. C **76**, 064317 (2007).
[18] F. Bečvář, Nucl. Instrum. Methods Phys. Res. A **417**, 434 (1998).
[19] R. Capote *et al.*, Nucl. Data Sheets **110**, 3107 (2009).
[20] A. J. Koning, S. Hilaire, and M. C. Duijvestijn, in *Proceedings of the International Conference on Nuclear Data for Science and Technology - ND2007*, edited by O. Bersillon *et al.* (EDP Sciences, Les Ulis, France, 2008), p. 211.
[21] T. Fuketa and J. A. Harvey, Nucl. Instrum. Methods **33**, 107 (1965).
[22] T. von Egidy and D. Bucurescu, Phys. Rev. C **80**, 054310 (2009).
[23] J. E. Lynn, *The Theory of Neutron Resonance Reactions* (Oxford University, Oxford, 1968).